Title of the paper:

Effect of treatment planning system parameters on beam modulation complexity for treatment plans with single-layer multi-leaf collimator and dual-layer stacked multi-leaf collimator

Shortened version:

Effects of TPS parameters on modulation complexity considering the MLC

Type of Manuscript:

Full paper / observational

Conflict of interest:

The authors declare no conflict of interest with respect to the present research

Abstract

Objective: High levels of beam modulation complexity (MC) and monitor units (MU) can compromise the plan deliverability of intensity-modulated radiotherapy treatments. Our study evaluates the effect of three treatment planning system (TPS) parameters on MC and MU using different multi-leaf collimator (MLC) architectures.

Methods: 192 volumetric-modulated arc therapy plans were calculated using one virtual prostate phantom considering three main settings: (1) three TPS-parameters (Convergence; Aperture Shape Controller, ASC; and Dose Calculation Resolution, DCR) selected from Eclipse v15.6, (2) four levels of dose-sparing priority for organs at risk (OAR), and (3) two treatment units with same nominal conformity resolution and different MLC architectures (Halcyon-v2 dual-layer MLC, DL-MLC & TrueBeam single-layer MLC, SL-MLC). We use seven complexity metrics to evaluate the MC, including two new metrics for DL-MLC, assessed by their correlation with gamma passing rate (GPR) analysis.

Results: DL-MLC plans demonstrated lower dose-sparing values than SL-MLC plans (p<0.05). TPS-parameters didn't change significantly the complexity metrics for either MLC architectures. However, for SL-MLC, significant variations of MU, target volume dose-homogeneity, and dose-spillage were associated with ASC and DCR (p<0.05). MU were found to be correlated (highly or moderately) with all complexity metrics (p<0.05) for both MLC plans. Additionally, our new complexity metrics presented a moderate correlation with GPR (r < 0.65). An important correlation was demonstrated between MC (plan deliverability) and dose-sparing priority level for DL-MLC.

Conclusions: TPS-parameters selected do not change MC for DL-MLC architecture, but they might have a potential use to control the MU, PTV homogeneity or dose spillage for SL-MLC. Our new DL-MLC complexity metrics presented important information to be considered in future pre-treatment quality assurance programs. Finally, the prominent dependence between plan deliverability and priority applied to OAR dose sparing for DL-MLC needs to be analysed and considered as an additional predictor of GPRs in further studies.

Advances in knowledge: Dose-sparing priority might influence in modulation complexity of DL-MLC.

Introduction

Beam modulation is a principal feature in advanced radiotherapy techniques using static field Intensity Modulation or Volumetric Modulated Arc-Therapy (VMAT). Due to the synchronised motion of the leaves of the

multi-leaf collimator (MLC) the radiation dose can be conformed to complex planning target volume (PTV) shapes, increasing the treatment effectiveness and keeping the adverse effects as low as possible by avoiding organs at risk (OARs) [1,2].

The Halcyon-v2 (Varian Medical Systems, Palo Alto, US) is a jaw-free linear accelerator (linac) that has a stacked-staggered MLC with two layers of leaves (distal and proximal to the linac target) offset by 5 mm. As described in the work of Cozzi et al. [3], each leaf has a 10 mm width projected at isocentre and has an effective conformity-resolution of 5 mm as a result of the overlap arrangement. Furthermore, the Halcyon-v2 (Hv2) allows independent displacements of the proximal and distal layers simultaneously, resulting in more modulation possibilities[3–8]. However, Lim et al. [4] found dose discrepancies between measured and calculated treatments, suggesting that high modulated beams can increase the leaf travelled-distance between the layers, allowing some distal leaf-edges to be exposed, increasing dose leakage within the leaf gaps.

The Treatment Planning System (TPS) is the software dedicated to the inverse optimisation process needed to generate VMAT treatment plans. This software has parameters that impact the final dose fluence by the hardware setting parameters such as MLC velocity, gantry speed, and dose rate[9–11]. Consequently, if these TPS parameters are not handled properly, treatments with challenging dose requirements may bring unrealistic or high demanding machine conditions (i.e., highly modulated plans), reducing accuracy of dose delivery[12,13].

Eclipse-v15.6 TPS (Varian Medical Systems, Palo Alto, U.S.) performs the inverse optimisation of VMAT plans with the Photon Optimiser (PO) algorithm[14]. The PO, based on a direct aperture optimization process, uses a multi-resolution (MR) approach with fast and periodical calculations of the dose distribution, starting with a lower number of dose calculation segments and initial MLC positions conforming to the target volume. When this optimisation is continued, and the MR level increases, the dose calculation segments also increase, interpolating the MLC positions to obtain new leaf apertures that correspond to the improved dose distribution. During the MR optimisation, the dose calculation accuracy increases as the number of dose segments increases with a maximum separation of 2-4 degrees, depending on the arc span[15].

The modulation complexity has been studied widely on linacs with single-layer MLC architecture, using metrics such as modulation index (MI)[16], modulation complexity score (MCS) [17], texture methods [18], dimensional fractal analysis[19], and aperture-based methods[20]. These complexity analyses have proven to be useful to compare linac performances between treatment techniques [5], to evaluate the best plan parameters in specific planning scenarios[20,21], to predict delivery accuracy [22], and to establish reference values for dosimetry audits[23].

The work reported by Park et al[24] and Antoine et al[25] summarises various modulation indices dedicated to predicting the plan-delivery accuracy in VMAT treatments. Similarly, the literature review by Chiavassa et al[26] includes all current complexity indices and the relevance of each metric. Recently, Tamura et al[27] propose the first modulation metric dedicated to dual-layer MLC (DL-MLC) architecture of Hv2, considering a weighted method using the distal and proximal layer contributions in the field conformation. However, none of the above-

mentioned studies investigates the influence of TPS parameters on beam modulation complexity, and most of them are focused on single-layer MLC (SL-MLC) architecture.

The primary aim of the present study was to investigate the effect of specific TPS-parameters on modulation complexity for VMAT treatments. The secondary aim was to determine if that effect is the same for different MLC architectures (DL-MLC or SL-MLC). Additionally, to evaluate the modulation complexity in the DL-MLC scenario, new complexity metrics were proposed considering the number of uncovered pair-leaves and the number of significant changes in leaves' positions, both presented in the beam modulation.

Methods

Plan configuration

Ninety-six VMAT plans were generated with Eclipse 15.6 using a single prostate patient dataset as a virtual phantom to deliver 2Gy per fraction in one full arc. The linac configuration was Hv2 with DL-MLC, maximum leaf speed of 50 mm/s, 6 MV flattening filter-free (FFF) photon beam, and a dose rate of 740 Gy/min. The same plans were replicated using the TrueBeam (TB) linac configuration with SL-MLC Millennium-120, maximum leaf speed of 25 mm/s, 6 MV FFF photon beam, a dose rate of 800 Gy/min, with jaw tracking mode turned off. For both cases, the plans were calculated with the anisotropic analytical algorithm (AAA) and were optimised with the PO algorithm, applying automatic mode for normal tissue objective and a structure optimisation resolution of 2.5 mm. Both treatment units were calibrated at the same reference conditions.

TPS parameters

The three studied parameters from Eclipse TPS features were Convergence (Conv), Aperture Shape Controller (ASC), and Dose Calculation Resolution (DCR), and their respective modes were Conv{off; on; extended}, ASC{off; low; moderate; very_high}, and DCR{normal; high}.

1. The Conv parameter controls the internal schedule of the transitions between and within the different multi-resolution (MR) levels of the PO. These changes in the transition times expect improved optimization results in dose fluence because the number of iteration increase, when modes= on/extended (respect the mode= off) by a factor of 2.5/11.2 on MR-1, 2.0/17.8 on MR-2, 1.0/17 on MR-3, and 1.0/15 on MR-4 for modes On/Extended respectively. However, the MU values may increase, and the optimisation time rises 1.2 - 3 fold for On mode, and a few hours for Extended mode[28]
2. The ASC parameter is a tool of the leaf-motion sequencer of the PO that penalises the leaf position deviations with respect to the adjacent leaves in the same continuous target projection. This penalty is introduced in the optimisation process, and its magnitude depends on the selected mode (Off, Very_low, Low, Moderate, high, and Very_high). Controlling the size and shape of the field with ASC may help to reduce the MU, the dose delivery inaccuracies, and the control quality failures [28]. For single-layer MLC architecture, Binny et al [29] found that ASC may be useful to improve the distribution of MU per degree throughout the treatment time, but it requires to evaluate its potential impact on treatment time. In our study, we limited the modes setting to: off, low, moderate and very_high, to evaluate the

impact of the parameter and differences in the obtained results between extremes (off and very_high) and small changes (low and moderate).

3. The DCR is a dose optimisation parameter related to the grid resolution of the internal dose calculation engine of PO [28]. The modes High (1.25 mm) and Normal (2.50 mm) of DCR change the internal grid size within each MR dose calculation, influencing the pre-calculated dose resolution, which impacts directly in the leaf sequencing, the dose rate, the MU/deg, and thus, the final dose distribution within the optimisation process.

Dose sparing Priority

To simplify the planning process, the OARs (OAR1: rectum, OAR2: bladder) were considered as independent structures to be avoided with no clinical differentiation between them. The avoidance was controlled by reducing their mean dose using the optimization objective upper_gEUD (from generalized Equivalent Uniform Dose) [30]. This optimization tool tries to reduce the volume that receives mid-dose levels (mean dose) using the parameter '*a*' that is set as 1 for parallel organs (following the rationale of Lyman-Kutcher-Burman NTCP model) [31–33]. This parameter *a* can take values up to 40 for serial organs minimizing the maximum dose contributions to the OAR. In this experiment, we supposed both OARs as parallel organs using *a*=1.

To counter the dependence of the same-patient dataset[23] and to consider possible effects of the TPS parameters over various dose-sparing scenarios, four levels of dose-sparing priorities for OARs were implemented within the optimization process. Priority values of 20, 40, 60, and 80 were selected to be applied with the upper_gEUD parameter, representing lower, moderate, high and very-high dose sparing conditions respectively. Contrastingly, a priority value of 100 was used with the dose coverage (100% of the prescription dose) and maximum dose (105% of prescription dose) parameters for the PTV, and for the maximum dose constraint for the whole-body structure

In total, 96 plans were produced, covering all permutations of the three TPS-parameters mode settings (four for ASC, three for Conv, and two for DCR), and four optimisation priority settings for the OAR mean dose constraint.

Plan quality indices

The metrics used to evaluate the plan quality were based on the recommendations of the International Commission on Radiation Units & Measurements (ICRU) Report 83[34]. We chose to use: the conformity index (CI), defined as the ratio between the volume that enclose the prescription dose (Vp) and the volume of PTV (VPTV), {CI= Vp / VPTV}; and the homogeneity index (HI), defined as the ratio between the dose difference that covers 98% and 2% of the volume (D98% and D2% respectively) and the prescription dose (Dp), {HI= (D2%-D98%) / Dp)}. Additionally, we recorded the mean dose of the PTV (mD-PTV), the volume enclosed by the 50% isodose (V50%) as a dose spillage metric, and the mean dose of OAR1 and OAR2 (mD-OAR*n*).

Complexity metrics

The complexity metrics used in this study are summarised, with their respective equations, in supplementary Table 1 (S-Table 1). These metrics were calculated using a Python script [35] that processes the information from DICOM-RT files[36,37], reading the leaves positions per CP with the Pydicom library[37]. The complexity metrics were the number of MU (**MU**)[38], the average MU increment by CP (**MUcp**)[38], the MCS for VMAT treatments (**MCSv**)[21],

and the weighted MCSv for DL-MLC architecture (**MCSw**)[27]. Additionally, we proposed two new complexity metrics and one adapted metric. They are the uncovered-layer score (**UL)**, the number of peaks score (**NP**) and the MCSw weighted by UL (**MCSUL)**, respectively.

The UL considers all leaf-pairs uncovered by their respective leaves from the complementary MLC layer (above or below). Figure 1 shows an example from an MLC sequence where the proximal layer leaves do not cover a distal leaf-pair section, creating an uncovered region that might increase the dose transmission, and thus, be related with dose measurements discrepancies due to incomplete attenuation of the beam[4]. This metric is calculated by summing the number of uncovered gaps per CP considering both, the distal and proximal layers. This sum is weighted by the relative fraction of MU in that CP (S-Table 1, Equation 9).

Figure 1. Uncovered leaves junction of the distal multi-leaf collimator (MLC) layer by the proximal MLC layer. This figure shows a conformed field in one control point (CP) from a specific treatment. The green and purple leaves differentiate the MLC banks (right and left).

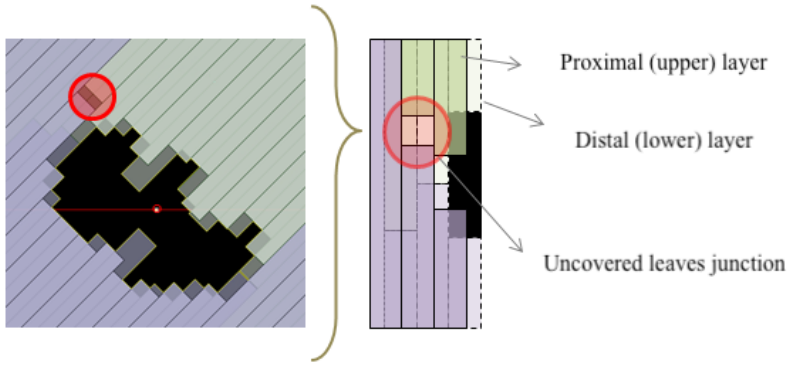

The proposed metric, NP, accounts for the modulation complexity (for SL-MLC or DL-MLC), calculating the average number of peaks presented in the trajectory profiles of all moving leaves in a VMAT treatment. As is shown in Figure 2, the position at each CP of a single leaf can be visualized within a trajectory profile, where the peaks represent significant changes in leaf speed and position. These variations can be associated with demanding hardware conditions that may generate dose delivery inaccuracies [39,40].

The metric, MCSUL, is an adapted version of MCSw[27], including UL as an additional factor to be considered in the complexity score of each MLC layer. Its calculation is described in Equations 10, 11 and 12 from S-Table 1.

Figure 2. Trajectory profile of the 30th leaf of TrueBeam (TB) from a prostate treatment plan labelled TB-plan_1. The red marks indicate the number of detected peaks using the function *find_peaks* from SciPy [41].

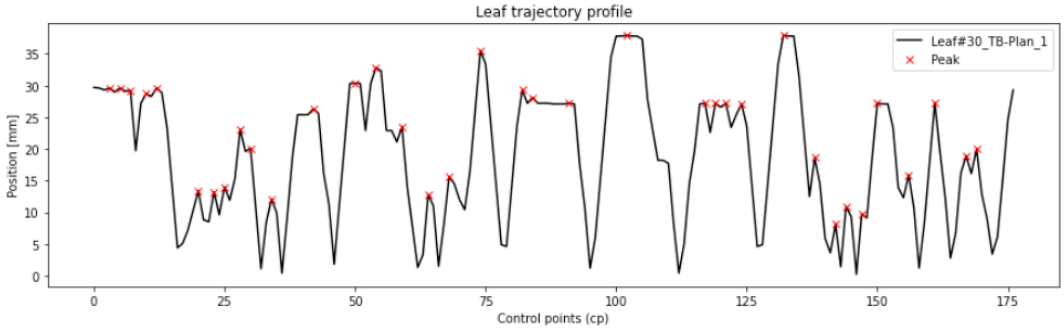

Complexity metrics validation

The new complexity metrics were introduced in this study to investigate the deliverability and quality of the plans produced with DL-MLC. To assess the value of these, they were compared with the gamma passing rate (GPR) calculated using gamma analysis[43].

To analyse the correlation of the new complexity metrics with GPR, the prostate plans for Hv2 were measured with the integrated electronic portal imaging device (EPID). The Hv2 EPID has a resolution of 1280x1280 pixels, 0.34 mm/pixel at the panel and 0.22 mm/pixel at isoplane, and a panel size of 43 cm x 43 cm [42]. Furthermore, the accuracy of dose delivery was evaluated with gamma analysis (γ) [43] using various levels for global dose difference (DD) of prescribed dose and distance to agreement (DTA) for at least 98% of all pixels. The DD/DTA levels were 3%/3 mm, 3%/2 mm, 2%/3 mm, 2%/2 mm, and 2%/1 mm. The images were processed using the portal dosimetry tool available in Eclipse 15.6, with the absolute absorbed dose correction and the improved gamma evaluation mode utilised.

In contrast with the Hv2, portal dosimetry on the TB with 6 MV-FFF mode is not possible in our institution due to the detector saturation and lack of an image prediction algorithm, depending on linac model used. For this reason and based on to the reported correlation between the MU values and the dose deliverability[18-29], the MU was selected as a reference index to compare the performance of each calculated complexity metric.

Statistical Analysis

The statistical significance of the correlations between the TPS-parameters, the complexity metrics and the gamma analysis were evaluated using Spearman's rank correlation coefficient (r) with a threshold of $p<0.05$ [24]. The low, moderate and high correlations were considered for values of $|r|<0.4$, $0.4\leq|r|\leq0.7$, and $|r|>0.7$ respectively [27,44]. The correlation between the modes of each TPS-parameter were tested for significance ($p<0.05$) using Wilcoxon signed-rank test.

Results:

After calculating the VMAT plans as described earlier, three main aspects were assessed for this study. First, as a general overview, the modulation complexity metrics and plan quality indices calculated for both linacs were compared. Second, the impact of each TPS-parameter mode on modulation complexity and plan quality were

evaluated, considering the MLC architecture. Finally, to verify the implications in plan deliverability, the correlations between the complexity metrics and MU, and between GPRs and the novel metrics for DL-MLC were evaluated.

To compare the performance between the two linacs/ MLC designs, Figure 3 presents the boxplots of all complexity metrics and plan quality indices that demonstrated a significant difference ($p<0.05$) between Hv2 and TB plans. It was found that Hv2 plans demonstrated lower values of V50%, mD-OAR1 (rectum), CI, MUcp, MCSv, and NP, compared to TB plans (Supplementary Table 2, S-Table 2). Additionally, it was noticed that TB plans presented more outliers, indicating less consistent results.

Figure 3. Boxplots of complexity metrics and plan quality indices that presented a significant difference between Halcyon-v2 (Hv2) and TrueBeam (TB) plans. The boxplot displays the minimum and maximum values of the data distribution indicated by the end of the whiskers; the lower and upper box limits are the first and third quartile; the horizontal line indicates the median value, and the red dot represents the mean value. Any additional point outside is considered as an outlier).

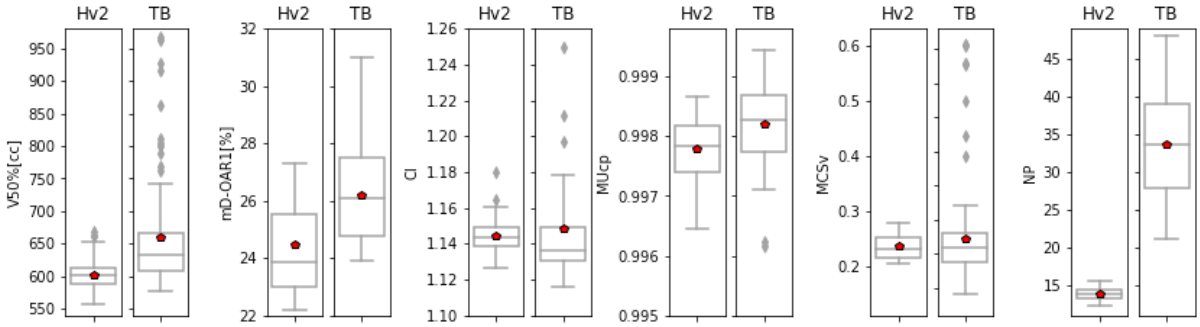

For each combination of TPS-parameter modes, the complexity scores and plan quality indices were compared using the Wilcoxon signed-rank test. Table 1 summarizes the parameter modes where significant changes were found. For Hv2 plans (DL-MLC) with Conv{off} were associated with slightly lower V50% values than Conv{extended}. However, the other TPS-parameters combinations did not influence the complexity nor the plan quality metrics significantly. In TB plans (SL-MLC), the CI, HI, mD-PTV, and V50%, demonstrated significant differences for parameters combinations including ASC and DCR (Table 1). Furthermore, significantly lower values of MU were required with ASC{off} compared to ASC{moderate}.

Table 1. Significant differences between the TPS-parameter modes on plan quality indices and complexity metrics for Hv2 and TB plans.

linac	Metric	Sample Size	TPS-parameter	Mean ± SD	p
Halcyon	V50% [cc]	32	Conv{Off}	597 ± 18	0.04
		32	Conv{Ext}	603 ± 24	
TrueBeam	CI	24	ASC{off}	1.14 ± 0.01	<0.01
		24	ASC{very_high}	1.15 ± 0.05	
		48	DCR{normal}	1.16 ± 0.06	<0.01
		48	DCR{high}	1.13 ± 0.02	
	HI	24	ASC{off}	0.10 ± 0.03	0.04
		24	ASC{very_high}	0.11 ± 0.05	
	mD-PTV	24	ASC{off}	105 ± 2	0.04
		24	ASC{moderate}	104 ± 2	
		24	ASC{low}	104 ± 2	<0.01
		24	ASC{very_high}	105 ±3	
	V50% [cc]	48	DCR{normal}	678 ± 101	<0.01
		48	DCR{high}	641 ± 54	
	MU	24	ASC{off}	802 ± 149	0.04
		24	ASC{moderate}	880 ± 134	

Abbreviations: TPS treatment planning system, Hv2 Halcyon-v2, TB TrueBeam, CI conformity index, HI homogeneity index, mD-PTV means dose of planning target volume, mD-OARn mean dose of OARn, V50% volume enclosed by the 50% isodose, ASC aperture shape controller, DCR dose calculation resolution, Conv convergence, SD standard deviation.

Figures 4 and 5 present scatterplots of all the complexity scores against required MU for Hv2 and TB plans, respectively. For Hv2 plans, required MU showed a high correlation to MCSv (I*r*I= 0.97), MCSw (I*r*I= 0.96), MUcp (I*r*I= 0.78), and NP (I*r*I= 0.76); and a moderate correlation to UL (I*r*I= 0.69) and MCSUL (I*r*I= 0.58). For TB plans, MU showed high correlation only to MCSv (I*r*I= 0.92). Additionally, a remarkable data clustering by the upper_gEUD priority values was demonstrated for Hv2 plans (Figure 4), which is not present in the case of TB (Figure 5)

Figure 4. Scatterplot of all complexity metrics for Hv2 plans using the MU values as the reference score and considering the effect of different levels of dose sparing priorities (upper_gEUD values).

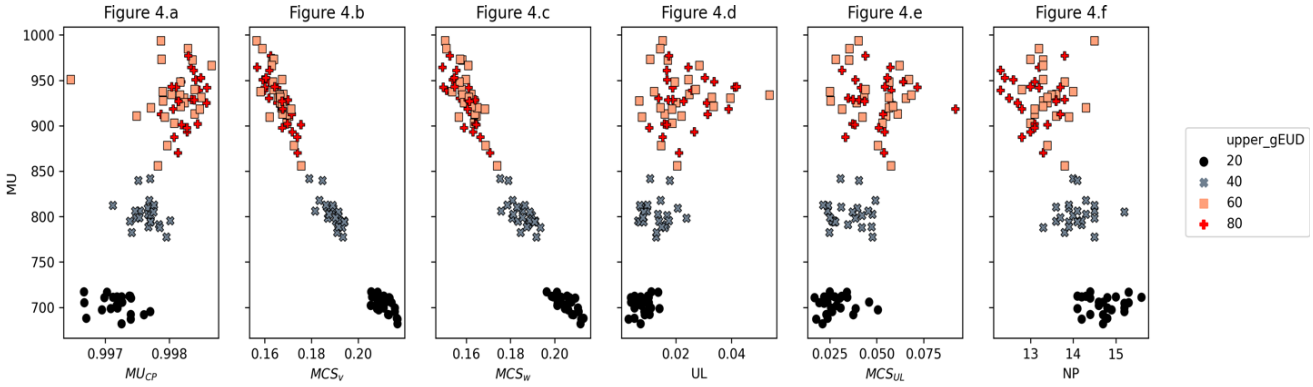

Abbreviations: Hv2 Halcyon-v2, MU monitor units, MUcp average MU increment by control point, MCSv modulation complexity score for volumetric modulated arc therapy, MCSw the weighted MCSv for dual-layer multi-leaf collimator architecture, UL uncover layer score, MCS_{UL} weighted MCSw by UL, NP number of peaks

Figure 5. Scatterplot of all complexity metrics for TB plans using the MU values as the reference score and considering the effect of different levels of dose sparing priorities (upper_gEUD values).

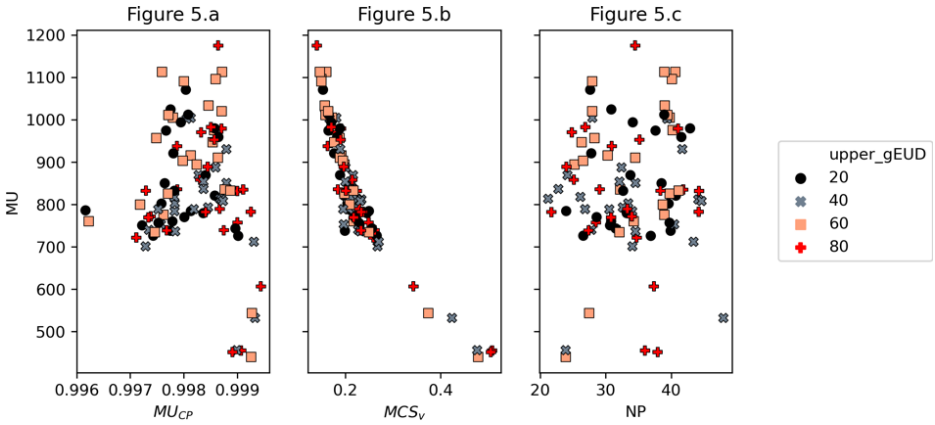

Abbreviations: TB TrueBeam, MU monitor units, MUcp average MU increment by CP, MCSv modulation complexity score for volumetric modulated arc therapy, NP number of peaks

The GPR's for evaluation criteria of 3%/3 mm, 3%/2 mm, and 2%/ 3mm were always 100% for all cases and thus, were not considered in the analysis (Supplementary Table 3, S-Table 3). The mean value and standard deviation (SD) for GPR with 2%/1 mm criteria were 96.3% and 1.7% respectively. Figure 6 shows the scatterplot of the complexity metrics against GPR, again plotted to indicate the associated upper_gEUD priority values. The GPR presented high correlation to MU, MCSv, and MCSw (|r|= 0.74, 0.74, and 0.72); moderate correlation to MUcp, UL, and NP (|r|= 0.66, 0.48, and 0.63); and low correlation to MCSUL. Additionally, the GPR present a similar clustering data effect as seen in Figure 4, with less differentiation for upper_gEUD priority values of 40, 60, and 80, compared to upper_gEUD values of 20.

Figure 6. Scatterplot of all complexity metrics from 96 prostate plans delivered on Halcyon-v2 (Hv2), considering the gamma passing rate (GPR) values. All cases presented low Pearson's correlation (|r|<0.4).

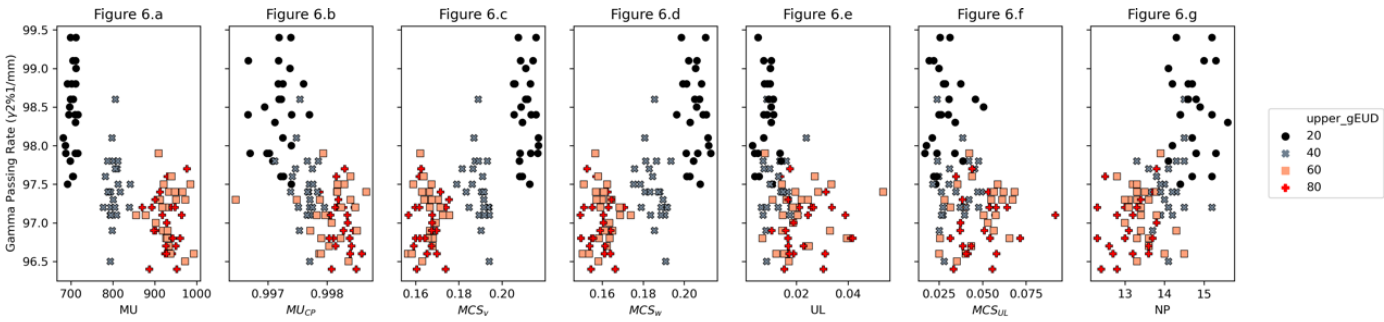

Discussion:

This *in silico* study investigated the possible effects of the selected TPS-parameters on different plan quality and modulation complexity metrics. At the same time, it was intended to evaluate if those effects are the same for treatments having different MLC architecture. Accordingly, three main aspects were considered to develop this research, (1) the TPS-parameters of ASC, DCR, and Conv were chosen because of their possible effects on the final dose fluence[28], (2) the selected linac configurations were Hv2 with DL-MLC and TB with SL-MLC, and (3) one prostate CT data set was used as a virtual phantom to control any effects attributable to differences in anatomy or planning volumes[23].

Figure 3 summarises the statistically significant differences observed in the plan quality indices and modulation complexity, comparing Hv2 and TB plans. It was found that Hv2 plans were associated with a higher median value of CI, better dose sparing contributions (lower V50%), and lower mean dose values in OAR1 (mD-OAR1) ($p<0.05$). As it is described in previous reports[5,42,45,46], these results can be attributed to the Hv2 features of lower penumbra (due to the leaf tip shape), higher leaf speed, lower dosimetric leaf gap, and higher gantry speed, compared to TB with Millennium-120 MLC. In the same way, it is important to note that these differences in features (hardware and beam modelling) make it impossible to directly compare the complexity metrics between the two linacs[23].

From Figure 3, it is also clear that metrics from Hv2 plans demonstrate less spread or variation than the data from TB plans. Furthermore, the TB data exhibits considerable outliers in the CI, V50%, and MCSv. We infer from this observation that the Hv2 plans (with DL-MLC) show more consistent outcomes or less sensitivity to the TPS parameters, than those for the TB configuration with SL-MLC. As we move towards the era of on-table adaptation[47–49], this reduced sensitivity to parameter variation may be an important feature regarding the requirement for rapid (high pressured) re-planning using either manual or automatic techniques, given both require some oversight and quality control (QC).

The results summarized in Table 1 demonstrate the selected TPS-parameters combinations do not impact the modulation complexity of plans with DL-MLC. Contrastingly, plans with SL-MLC presented lower MU values for treatments with ASC{off} decreasing the plan complexity[26] (Figure 5). For Hv2 plans, only the comparison between Conv{off} and Conv{extended} demonstrated a statistically significant difference in the V50% metric. Interestingly, with the mode set to “off”, a lower mean V50% value was obtained; however, this reflected the narrower range of values achieved for this parameter settings compared to the “extended” mode. Thus, although the difference was significant, it is important to note that these variations may not represent considerable clinical differences.

For TB plans, the same scenario (low variations) happened to the CI, HI, and mD-PTV metrics. Moreover, lower values of V50% (achieved by DCR{high}) and MU (achieved by ASC{off}) presented relevant changes that might impact the plan quality and dose deliverability[26,27]. Nevertheless, the statistical significance needs to be careful considered in each particular case because each mode has different plans depending on their respective TPS-parameter. For instance, ASC with four modes has 24 plans each, whilst DCR (two modes) has 48 plans.

Figure 4 shows the correlation of all modulation complexity metrics with MU for Hv2 plans. Aside from the strong correlation seen in the Hv2 data, a clear grouping level is evident with the priority settings used with the upper_gEUD optimisation constraint. For each of the plots (the different modulation) the data groups to the lower (20), moderate (40) and high/very-high (60/80) priority settings for the dose sparing parameter. These well-differentiated regions suggest a strong dependence between the modulation complexity degree (measured in 7 different ways), and the priority levels used to reduce the mean dose of OARs in the optimization process, therefore, providing an opportunity to "pre-select" the required range of solution in terms of acceptable complexity. These results showed that high demanding dose sparing conditions might generate plans with higher MU values, with more complex modulation (lower values of MCSv and MCSw), with higher number of uncovered leaves junction per CP (UL), but at the same time with a lower number of demanding changes in the leaf position throughout the modulation process (NP), albeit a small effect of the latter.

Figure 5, showing the same analysis for the TB plans, does not show such a strong correlation, nor grouping. It is likely that the latter reflects the weaker overall correlation and the wider range of plan metrics previously highlighted. Comparison of the corresponding plots in figures 4 and 5 suggests again that the variation of the treatment planning parameter modes has a smaller effect on the plans produced for the Halcyon model over that for the TrueBeam. This is particularly apparent in the behaviour seen in Figure 5c, where a much greater heterogeneity is seen in the data. The large variation in Numbers of Peaks seen in the leaf trajectories suggest an 'unstable' relationship between the leaf sequences generated and parameter variation. In turn this indicates the 'TrueBeam' optimisation search space is far more complex and poorly behaved, with many local minima, leading to these spreads of 'optimal' solutions. This should not be taken as a reason to distrust the algorithms; however, it does emphasize the need for caution, QC and oversight of the planning process.

The different behaviour shown in Figures 4 and 5, suggests that Photon Optimiser might work differently for the two Linac/ MLC models when the optimization priorities are used to reduce the OAR mean dose. In general terms, it was expected that more demanding plans (with higher dose sparing priorities) would require more complex beam modulation with higher MU values. This was evident in the results seen for Hv2 cases, however for TB plans, it seems to be uncorrelated; suggesting that a common optimization template could not be expected to produce similar results for the different Linac/MLC models. Nevertheless, this behaviour needs to be analysed in further investigations considering other optimization parameters used to control the dose of OARs and the potential impact on dose deliverability.

Finally, Figure 6 considered the correlation between the novel modulation complexity scores and the Gamma Passing Rate (GPR), taking the latter as a measure of dose deliverability. The analysis showed a moderate correlation to GPR (UL and NP). However, they account for physical aspects, which impact the delivered dose, that other published metrics do not[26] and it would be valuable to include them (or superior versions) in treatment verification programs[47]. However, again a clear clustering of the data with dose

limiting priority value is evident and suggests a simple connection between driving the optimiser harder (higher priority) and obtaining more complex solutions (higher MU, MUCP and lower MCSV, MCSW, NP) which intuitively challenge attaining a maximum GPR. In Figures 6a, 6b and 6c, the clustering is strong, however for the novel metrics proposed herein the grouping is less of more diffuse. Specially, the Uncovered Layers (UL) have a potential impact in plans evaluation with dose delivery inaccuracies due to high inter-leaves dose contributions that are not considered by the TPS[4]. To achieve a better understanding of these new metrics, it is necessary to validate them using different target volumes, anatomic regions, and dose prescription.

Conclusions

This work demonstrated that when the selected treatment planning system parameters were systematically varied, plans created for the Halcyon beam model (in Eclipse) demonstrated much less variation in the scoring metrics (plan quality and modulation complexity) than those generated in the same planning system for TrueBeam. A strong clustering, by OAR mean dose limiting priority setting, in the correlation between the quality and modulation complexity scores was demonstrated within the Halcyon plans. Furthermore, the new metrics dedicated to DL-MLC propose novel tools to be used and included in the analysis of pre-treatment quality assurance programs.

References

1. Semenenko VA, Li XA. Lyman–Kutcher–Burman NTCP model parameters for radiation pneumonitis and xerostomia based on combined analysis of published clinical data. Physics in Medicine and Biology [Internet]. 2008 Feb 7 [cited 2019 Nov 7];53(3):737–55. Available from: http://stacks.iop.org/0031-9155/53/i=3/a=014?key=crossref.21b843885a46d494ab5621e962108314
2. Wu Z, Xie C, Hu M, Han C, Yi J, Zhou Y, et al. Dosimetric benefits of IMRT and VMAT in the treatment of middle thoracic esophageal cancer: is the conformal radiotherapy still an alternative option? Journal of Applied Clinical Medical Physics [Internet]. 2014 May 1 [cited 2020 Apr 18];15(3):93–101. Available from: http://doi.wiley.com/10.1120/jacmp.v15i3.4641
3. Cozzi L, Fogliata A, Thompson S, Franzese C, Franceschini D, de Rose F, et al. Critical Appraisal of the Treatment Planning Performance of Volumetric Modulated Arc Therapy by Means of a Dual Layer Stacked Multileaf Collimator for Head and Neck, Breast, and Prostate. Technology in cancer research & treatment [Internet]. 2018 [cited 2020 Jan 10];17:1533033818803882. Available from: http://www.ncbi.nlm.nih.gov/pubmed/30295172
4. Lim TY, Dragojevic I, Hoffman D, Flores-Martinez E, Kim G. Characterization of the Halcyon TM multileaf collimator system. Journal of Applied Clinical Medical Physics [Internet]. 2019 Apr 19 [cited 2019 Nov 19];20(4):106–14. Available from: https://onlinelibrary.wiley.com/doi/abs/10.1002/acm2.12568
5. Petroccia HM, Malajovich I, Barsky AR, Ghiam AF, Jones J, Wang C, et al. Spine SBRT With Halcyon Plan Quality, Modulation Complexity, Delivery Accuracy, and Speed. Frontiers in oncology [Internet]. 2019 [cited 2019 Nov 15];9:319. Available from: http://www.ncbi.nlm.nih.gov/pubmed/31106151
6. Li T, Irmen P, Liu H, Shi W, Alonso-Basanta M, Zou W, et al. Dosimetric Performance and Planning/Delivery Efficiency of a Dual-Layer Stacked and Staggered MLC on Treating Multiple Small Targets: A Planning Study Based on Single-Isocenter Multi-Target Stereotactic Radiosurgery (SRS) to Brain Metastases. Frontiers in Oncology [Internet]. 2019 Jan 22 [cited 2019 Nov 21];9:7. Available from: https://www.frontiersin.org/article/10.3389/fonc.2019.00007/full
7. Lloyd SAM, Lim TY, Fave X, Flores-Martinez E, Atwood TF, Moiseenko V. TG-51 reference dosimetry for the Halcyon: A clinical experience. Journal of Applied Clinical Medical Physics [Internet]. 2018 Jul 1 [cited 2019 Nov 19];19(4):98–102. Available from: http://doi.wiley.com/10.1002/acm2.12349

8. Gay SS, Netherton TJ, Cardenas CE, Ger RB, Balter PA, Dong L, et al. Dosimetric impact and detectability of multi-leaf collimator positioning errors on Varian Halcyon. Journal of Applied Clinical Medical Physics [Internet]. 2019 Aug 11 [cited 2019 Nov 15];20(8):47–55. Available from: https://onlinelibrary.wiley.com/doi/abs/10.1002/acm2.12677
9. Liu H, Sintay B, Pearman K, Shang Q, Hayes L, Maurer J, et al. Comparison of the progressive resolution optimizer and photon optimizer in VMAT optimization for stereotactic treatments. Journal of Applied Clinical Medical Physics [Internet]. 2018 Jul 1 [cited 2020 Apr 18];19(4):155–62. Available from: http://doi.wiley.com/10.1002/acm2.12355
10. Tol JP, Dahele M, Peltola J, Nord J, Slotman BJ, Verbakel WF. Automatic interactive optimization for volumetric modulated arc therapy planning. Radiation Oncology [Internet]. 2015 Dec 1 [cited 2019 Nov 18];10(1):75. Available from: https://ro-journal.biomedcentral.com/articles/10.1186/s13014-015-0388-6
11. Shende R, Gupta G, Patel G, Kumar S. Assessment and performance evaluation of photon optimizer (PO) vs. dose volume optimizer (DVO) for IMRT and progressive resolution optimizer (PRO) for RapidArc planning using a virtual phantom. International Journal of Cancer Therapy and Oncology [Internet]. 2016 Sep 7 [cited 2019 Nov 18];4(3). Available from: http://www.ijcto.org/index.php/IJCTO/article/view/ijcto.43.7
12. Binny D, Kairn T, Lancaster CM, Trapp J v., Crowe SB. Photon optimizer (PO) vs progressive resolution optimizer (PRO): a conformality- and complexity-based comparison for intensity-modulated arc therapy plans. Medical Dosimetry [Internet]. 2018 Sep 1 [cited 2019 Nov 15];43(3):267–75. Available from: https://www.sciencedirect.com/science/article/abs/pii/S0958394717301140
13. Sanford L, Pokhrel D. Improving treatment efficiency via photon optimizer (PO) MLC algorithm for synchronous single-isocenter/multiple-lesions VMAT lung SBRT. Journal of Applied Clinical Medical Physics [Internet]. 2019 Oct 20 [cited 2019 Nov 19];20(10):201–7. Available from: https://onlinelibrary.wiley.com/doi/abs/10.1002/acm2.12721
14. Otto K. Volumetric modulated arc therapy: IMRT in a single gantry arc. Medical Physics [Internet]. 2008 [cited 2020 Oct 13];35(1):310–7. Available from: https://pubmed.ncbi.nlm.nih.gov/18293586/
15. Varian Medical Systems. Eclipse Photon and Electron Reference Guide. 2017. 263–348.
16. S W. Use of a quantitative index of beam modulation tocharacterize dose conformality: illustration by acomparison of full beamlet IMRT, few-segment IMRT(fsIMRT) and conformal unmodulated radiotherapy. Physics in Medicine & Biology [Internet]. 2003 [cited 2020 Mar 26];48(14):2051–62. Available from: https://www.researchgate.net/publication/280869940
17. McNiven AL, Sharpe MB, Purdie TG. A new metric for assessing IMRT modulation complexity and plan deliverability. Medical Physics [Internet]. 2010 Jan 12 [cited 2019 Nov 15];37(2):505–15. Available from: http://www.ncbi.nlm.nih.gov/pubmed/20229859
18. Park S-Y, Kim IH, Ye S-J, Carlson J, Park JM. Texture analysis on the fluence map to evaluate the degree of modulation for volumetric modulated arc therapy. Medical Physics [Internet]. 2014 Oct 31 [cited 2019 Dec 12];41(11):111718. Available from: http://doi.wiley.com/10.1118/1.4897388
19. Tambasco M, Nygren I, Yorke-Slader E, Villarreal-Barajas JE. FracMod: A computational tool for assessing IMRT field modulation. Physica Medica [Internet]. 2013 Sep 1 [cited 2019 Dec 12];29(5):537–44. Available from: https://www.sciencedirect.com/science/article/pii/S1120179712002037?via%3Dihub
20. Du W, Cho SH, Zhang X, Hoffman KE, Kudchadker RJ. Quantification of beam complexity in intensity-modulated radiation therapy treatment plans. Medical Physics [Internet]. 2014 Jan 21 [cited 2020 Sep 21];41(2):021716. Available from: http://doi.wiley.com/10.1118/1.4861821
21. Masi L, Doro R, Favuzza V, Cipressi S, Livi L. Impact of plan parameters on the dosimetric accuracy of volumetric modulated arc therapy. Medical Physics [Internet]. 2013 Jun 18 [cited 2019 Nov 15];40(7):071718. Available from: http://www.ncbi.nlm.nih.gov/pubmed/23822422
22. Valdes G, Solberg TD, Heskel M, Ungar L, Simone CB. Using machine learning to predict radiation pneumonitis in patients with stage I non-small cell lung cancer treated with stereotactic body radiation therapy. Physics in Medicine and Biology [Internet]. 2016 Aug 21 [cited 2019 Nov 5];61(16):6105–20. Available from: http://stacks.iop.org/0031-9155/61/i=16/a=6105?key=crossref.ac429b395960e79f413858fa12df82c9
23. McGarry CK, Agnew CE, Hussein M, Tsang Y, McWilliam A, Hounsell AR, et al. The role of complexity metrics in a multi-institutional dosimetry audit of VMAT. The British Journal of Radiology [Internet]. 2016 Jan 19 [cited 2020 Mar 22];89(1057):20150445. Available from: http://www.birpublications.org/doi/10.1259/bjr.20150445

24. Park JM, Kim J, Park S. Modulation indices and plan delivery accuracy of volumetric modulated arc therapy. Journal of Applied Clinical Medical Physics [Internet]. 2019 Apr 30 [cited 2019 Dec 12];20(6):acm2.12589. Available from: https://onlinelibrary.wiley.com/doi/abs/10.1002/acm2.12589
25. Antoine M, Ralite F, Soustiel C, Marsac T, Sargos P, Cugny A, et al. Use of metrics to quantify IMRT and VMAT treatment plan complexity: A systematic review and perspectives. Physica Medica [Internet]. 2019 Aug 1 [cited 2020 Jul 29];64:98–108. Available from: https://doi.org/10.1016/j.ejmp.2019.05.024
26. Chiavassa S, Bessieres I, Edouard M, Mathot M, Moignier A. Complexity metrics for IMRT and VMAT plans: a review of current literature and applications. The British Journal of Radiology [Internet]. 2019 Oct 24 [cited 2019 Dec 12];92(1102):20190270. Available from: https://www.birpublications.org/doi/10.1259/bjr.20190270
27. Tamura M, Matsumoto K, Otsuka M, Monzen H. Plan complexity quantification of dual-layer multi-leaf collimator for volumetric modulated arc therapy with Halcyon linac. Physical and Engineering Sciences in Medicine [Internet]. 2020 Jul 9 [cited 2020 Sep 2]; Available from: http://link.springer.com/10.1007/s13246-020-00891-2
28. Varian Medical Systems. TPS New Features Workbook v15.6. 2018.
29. Binny D, Spalding M, Crowe SB, Jolly D, Kairn T, Trapp J v., et al. Investigating the use of aperture shape controller in VMAT treatment deliveries. Medical Dosimetry. 2020 Mar 26;
30. Niemierko A. A generalized concept of equivalent uniform dose (EUD). Medical Physics. 1999;26(6):1100.
31. Fogliata A, Thompson S, Stravato A, Tomatis S, Scorsetti M, Cozzi L. On the gEUD biological optimization objective for organs at risk in Photon Optimizer of Eclipse treatment planning system. Journal of applied clinical medical physics [Internet]. 2018 Jan [cited 2019 Nov 21];19(1):106–14. Available from: http://www.ncbi.nlm.nih.gov/pubmed/29152846
32. Tsougos I, Mavroidis P, Theodorou K, Rajala J, Pitkänen MA, Holli K, et al. Clinical validation of the LKB model and parameter sets for predicting radiation-induced pneumonitis from breast cancer radiotherapy. Physics in Medicine and Biology [Internet]. 2006 Feb 7;51(3):L1–9. Available from: http://stacks.iop.org/0031-9155/51/i=3/a=L01?key=crossref.fb43d1eb75266dcb6acb4afbd92add55
33. Luxton G, Keall PJ, King CR. A new formula for normal tissue complication probability (NTCP) as a function of equivalent uniform dose (EUD). Physics in medicine and biology [Internet]. 2008 Jan 7 [cited 2020 Mar 31];53(1):23–36. Available from: http://www.ncbi.nlm.nih.gov/pubmed/18182685
34. Grégoire V, Mackie TR. State of the art on dose prescription, reporting and recording in Intensity-Modulated Radiation Therapy (ICRU report No. 83). Cancer radiotherapie : journal de la Societe francaise de radiotherapie oncologique [Internet]. 2011 Oct [cited 2020 Mar 30];15(6–7):555–9. Available from: http://www.ncbi.nlm.nih.gov/pubmed/21802333
35. Quintero P. pquinterome/MCS-calculation: Calculating the MCS for VMAT based on:" Masiet al. : Plan parameters and VMAT dosimetric accuracy - 2013" [Internet]. Github. 2020 [cited 2020 Jul 27]. Available from: https://github.com/pquinterome/MCS-calculation
36. Law MYY, Liu B. DICOM-RT and Its Utilization in Radiation Therapy. RadioGraphics [Internet]. 2009 May [cited 2020 Jan 27];29(3):655–67. Available from: http://pubs.rsna.org/doi/10.1148/rg.293075172
37. NEMA. PS3.3 [Internet]. [cited 2020 Jan 27]. Available from: http://dicom.nema.org/medical/dicom/current/output/html/part03.html
38. Tamura M, Monzen H, Matsumoto K, Kubo K, Otsuka M, Inada M, et al. Mechanical performance of a commercial knowledge-based VMAT planning for prostate cancer. Radiation Oncology [Internet]. 2018 Aug 31 [cited 2020 Oct 24];13(1):163. Available from: https://ro-journal.biomedcentral.com/articles/10.1186/s13014-018-1114-y
39. Kielar KN, Mok E, Hsu A, Wang L, Luxton G. Verification of dosimetric accuracy on the TrueBeam STx: Rounded leaf effect of the high definition MLC. Medical Physics [Internet]. 2012 Oct 1 [cited 2019 Nov 22];39(10):6360–71. Available from: http://doi.wiley.com/10.1118/1.4752444
40. Agnew A, Agnew CE, Grattan MWD, Hounsell AR, McGarry CK. Monitoring daily MLC positional errors using trajectory log files and EPID measurements for IMRT and VMAT deliveries. Physics in Medicine and Biology. 2014 May 7;59(9).
41. Scipy. scipy.signal.peak_prominences — SciPy v1.3.1 Reference Guide [Internet]. [cited 2020 Mar 30]. Available from: https://docs.scipy.org/doc/scipy-1.3.1/reference/generated/scipy.signal.peak_prominences.html#scipy.signal.peak_prominences
42. Kim H, Huq MS, Lalonde R, Houser CJ, Beriwal S, Heron DE. Early clinical experience with varian halcyon V2 linear accelerator: Dual-isocenter IMRT planning and delivery with portal dosimetry for gynecological cancer treatments. Journal of Applied Clinical Medical Physics [Internet]. 2019 Nov 29

[cited 2019 Dec 10];20(11):111–20. Available from: https://onlinelibrary.wiley.com/doi/abs/10.1002/acm2.12747
43. Low DA, Harms WB, Mutic S, Purdy JA. A technique for the quantitative evaluation of dose distributions. Medical Physics [Internet]. 1998 May 1 [cited 2020 Jul 27];25(5):656–61. Available from: http://doi.wiley.com/10.1118/1.598248
44. Mukaka MM. Statistics corner: A guide to appropriate use of correlation coefficient in medical research. Malawi Medical Journal. 2012;24(3):69–71.
45. Li C, Chen J, Zhu J, Gong G, Tao C, Li Z, et al. Plan quality comparison for cervical carcinoma treated with Halcyon and Trilogy intensity-modulated radiotherapy. Journal of Cancer [Internet]. 2019 [cited 2019 Dec 12];10(24):6135–41. Available from: http://www.ncbi.nlm.nih.gov/pubmed/31762823
46. Flores-Martinez E, Kim G, Yashar CM, Cerviño LI. Dosimetric study of the plan quality and dose to organs at risk on tangential breast treatments using the Halcyon linac. Journal of Applied Clinical Medical Physics [Internet]. 2019 Jun 11 [cited 2019 Dec 10];20(7):acm2.12655. Available from: https://onlinelibrary.wiley.com/doi/abs/10.1002/acm2.12655
47. Sonke J-J, Aznar M, Rasch C. Adaptive Radiotherapy for Anatomical Changes. Seminars in Radiation Oncology [Internet]. 2019 Jul [cited 2019 Nov 14];29(3):245–57. Available from: https://linkinghub.elsevier.com/retrieve/pii/S1053429619300165
48. Brock KK. Adaptive Radiotherapy: Moving Into the Future. Seminars in Radiation Oncology [Internet]. 2019 Jul 1 [cited 2019 Nov 14];29(3):181–4. Available from: https://www.sciencedirect.com/science/article/pii/S1053429619300207#fig0001
49. Ray X, Kaderka R, Hild S, Cornell M, Moore KL. Framework for Evaluation of Automated Knowledge-Based Planning Systems Using Multiple Publicly Available Prostate Routines. Practical Radiation Oncology. 2020;10(2).